International Tables for Crystallography (2006). Vol. C, Section 2.7.1, pp. 113–114.

2.7. Topography

BY A. R. LANG

2.7.1. Principles

The term diffraction topography covers techniques in which images of crystals are recorded by Bragg-diffracted rays issuing from them. It can be arranged at will for these rays to produce an image of a surface bounding the crystal, or of a thin slice cutting through the crystal, or of the projection of a selected volume of the crystal. The majority of present-day topographic techniques aim for as high a spatial resolution as possible in their point-by-point recording of intensity in the diffracted rays. In principle, any position-sensitive detector with adequate spatial resolution could be employed for recording the image. Photographic emulsions are most widely used in practice. In the following accounts of the various diffraction geometries developed for topographic experiments, the term 'film' will be used to stand for photographic emulsion coated on film or on glass plate, or for any other position-sensitive detector, either integrating or capable of real-time viewing, that could serve instead of photographic emulsion. (Position-sensitive detectors, TV cameras, and storage phosphors are described in Sections 7.1.6, 7.1.7, and 7.1.8.) All diffraction geometries described with reference to an X-ray source could in principle be used with neutron radiation of comparable wavelength (see Chapter 4.4).

Two factors, often largely independent and experimentally distinguishable, determine the intensity that reaches each point on the topograph image. The first is simply whether or not the corresponding point in the specimen is oriented so that some rays within the incident beam impinging upon it can satisfy the Bragg condition. The intensity of the Bragg-reflected rays will range between maximum and minimum values depending upon how well that condition is satisfied. The consequent intensity variation from point to point on the image is called *orientation contrast*, and it can be analysed to provide a map of lattice misorientations in the specimen. The sensitivity of misorientation measurement is controllable over a wide range by appropriate choice of diffraction geometry, as will be explained below. The second factor determining the diffracted intensity is the lattice perfection of the crystal. In this case, physical factors such as X-ray wavelength, specimen absorption, and structure factor of the active Bragg reflection fix the range within which the diffracted intensity can lie. One limit corresponds to the case of the *ideally perfect crystal*. This is a well defined entity, and its diffraction behaviour is well understood [see *IT* B (1996, Part 5)]. The other limit is that of the *ideally imperfect crystal*, a less precisely defined entity, but which, for practical purposes, may be taken as a crystal exhibiting negligible primary and secondary extinction. The magnitude, and sometimes also the sign, of the difference in intensity recorded from volume elements of ideally perfect as opposed to ideally imperfect crystals is to a large degree controllable by the choice of experimental parameters (in particular by choice of wavelength). Contrast on the topograph image arising from point-to-point differences in lattice perfection of the specimen crystal was called *extinction contrast* in earlier X-ray topographic work, but is now more usually called *diffraction contrast* to conform with terminology used in transmission electron microscopic observations of lattice defects, experiments which have many analogies with the X-ray case.

Figs. 2.7.1.1 and 2.7.1.2, respectively, show in plan view the simplest arrangements for taking a *reflection* topograph and a *transmission* topograph. The source of X-rays is shown as being point-like at S. If its wavelength spread is large then the Bragg condition may be satisfied over the whole length CD for Bragg planes oriented parallel to BB', and an image of CD will be formed on F by the Bragg-diffracted rays falling on it. The specimen is mounted on a rotatable axis (the ω axis) perpendicular to the plane of the drawing, which represents the median plane of incidence, in order that the angle of incidence on the planes BB' can be varied. The specimen is usually adjusted so that the diffraction vector, $\mathbf{h}$, of the Bragg reflection of principal interest is perpendicular to the ω axis. Let the mean source-to-specimen and specimen-to-film distances be a and b, respectively. Suppose the source S is extended a distance s in the axial direction (*i.e.* perpendicular to the plane of incidence). Then diffracted rays from any point on CD will be spread on F over a distance $s(b/a)$ in the axial direction. This is the simple expression for the axial resolution of the topograph given by ray optics. Transmission topographs have the value of showing defects within the interior of specimens, which may be optically opaque, but are in practice limited to a specimen thickness, t, such that μt is less than a few units (μ being the normal linear absorption coefficient) unless the specimen structure and the perfection are such as to allow strong anomalous transmission [the Borrmann effect, see *IT* B (1996, Part 5)]. If a reflection topograph specimen is a nearly perfect crystal then the volume of crystal contributing to the image is restricted to a depth below the surface given approximately by the X-ray extinction distance, ξ_h, of the active Bragg reflection, which may be only a few micrometres, rather than the penetration distance, μ^{-1}, of the radiation used.

Besides the ratio b/a, other important experimental parameters are the degree of collimation of the incident beam and its wavelength spread. The manner in which X-ray topographs exhibit *orientation contrast* and *diffraction contrast* under different choices of these parameters is illustrated schematically in Fig. 2.7.1.3. There, (*a*) represents a hypothetical specimen consisting of a matrix of perfect crystal C in which are embedded two islands A and B whose lattices differ from C in the following respects. A has the same mean orientation as C but is a region of

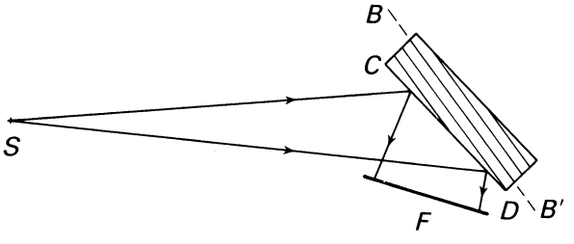

Fig. 2.7.1.1. Surface reflection topography with a point source of diverging continuous radiation.

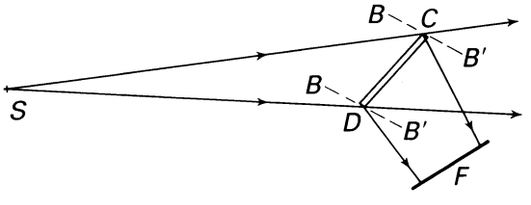

Fig. 2.7.1.2. Transmission topography with a point source of diverging continuous radiation.

high imperfection. (In reflection topographs, imperfect regions will always produce stronger *integrated* reflections than perfect regions and will also do so in transmission topographs under low-absorption conditions.) The island B is assumed to be as perfect as C, but is slightly misoriented with respect to C. The topograph images sketched in (b)–(e) could represent either reflection topographs or transmission topographs from a specimen thin compared with the dimension CD in Fig. 2.7.1.2. [Possible distortion of the images relative to the shape of (a) is neglected: this matter is considered later.] First, suppose that continuous radiation is emitted from the source S. If the ratio b/a is quite small, the topograph image will resemble (b). The island A is detected by diffraction contrast whereas island B will not show any area contrast since by assumption the incident radiation contains wavelengths enabling B to satisfy the Bragg condition just as well as C. The low-angle B–C boundary may show up, however, since it contains dislocations that will produce diffraction contrast and might be individually resolvable with a high-resolution topographic technique. Orientation contrast of B becomes manifest when b is increased, and measurement of the misorientation is then possible from the displacement of the image of B [as shown in (c)] consequent upon the different direction of Bragg-reflected rays issuing from it compared with those from C.

Next, suppose that S emits a limited range of wavelengths, *e.g.* characteristic $K\alpha$ radiation, and let the incident beam be collimated to have an angular spread in the plane of incidence that is smaller than the component in that plane of the misorientation between B and C, but larger than the angular range of reflection of C or A. Then, if the specimen is rotated about the ω axis so that A and C satisfy the Bragg condition, B will not do so and the topograph will resemble (d). [Island A shows up in (d) by diffraction contrast, as in (b).]. Appropriate rotation of the specimen will bring B into the Bragg-reflecting orientation, but will eliminate reflection from A and C, as shown in (e). The images (d) and (e) will not undergo significant change with variation in the ratio b/a, except for loss of resolution as b/a increases. The sensitivity of misorientation measurement will increase as the angular and wavelength spread of the incident beam are reduced, but when the angular range of a monochromatic incident beam is lowered to a value comparable with the angular range of reflection of the perfect crystal (generally only a few seconds of arc), it will not be possible with one angular setting alone to obtain an image that will distinguish between diffraction contrast and orientation contrast in the clear way shown in (d). The distinction will require comparison of a series of topographs obtained during a step-wise sweep of the angular range of reflection by the specimen. This is the procedure adopted in double-crystal or multicrystal topography, as described in Sections 2.7.3 and Subsection 2.7.4.2.

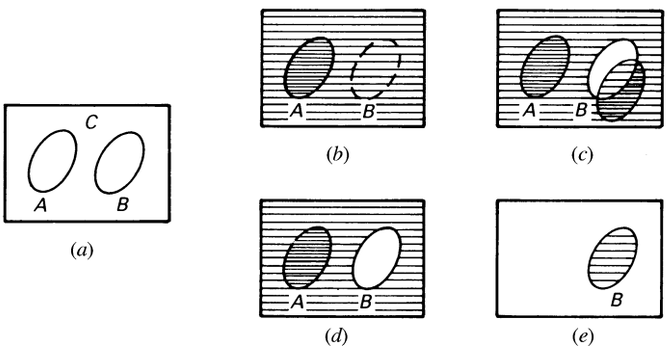

Fig. 2.7.1.3. Differentiation between orientation contrast and diffraction contrast in types of topograph images, (b)–(e), of a crystal surface (a).

Details concerning diverse variants in diffraction geometry used in X-ray topographic experiments, treatments of the diffraction contrast theory underlying X-ray topographic imaging of lattice defects, and listings of applications of X-ray topography can be found in reviews and monographs of which a selection follows. All aspects of X-ray topography are covered in the survey edited by Tanner & Bowen (1980). Armstrong & Wu (1973), Tanner (1976), and Lang (1978) describe experimental techniques and review their applications. The dynamical-diffraction theoretical basis of X-ray topography is emphasized by Authier (1970, 1977). Kato (1974) and Pinsker (1978) deal comprehensively with X-ray dynamical diffraction theory, which is also the topic of Part 5 of *IT* B (1996). Introductions to this theory have been presented by Batterman & Cole (1964), Hart (1971), and Hildebrandt (1982), the latter two being especially relevant to X-ray topography.

2.7.2. Single-crystal techniques

2.7.2.1. *Reflection topographs*

Combining the simple diffraction geometry of Fig. 2.7.1.1 with a laboratory microfocus source of continuous radiation offers a simple yet sensitive technique for mapping misorientation textures of large single crystals (Schulz, 1954). One laboratory X-ray source much used produces an apparent size of S 30 μm in the axial direction and 3 μm in the plane of incidence. Smaller source sizes can be achieved with X-ray tubes employing magnetic focusing of the electron beam. Then b/a ratios between $\frac{1}{2}$ and 1 can be adopted without serious loss of geometric resolution, and, with $a = 0.3$ m typically, misorientation angles of $10''$ can be measured on images of the type (c) in Fig. 2.7.1.3. The technique is most informative when the crystal is divided into well defined subgrains separated by low-angle boundaries, as is often the case with annealed melt-grown crystals. On the other hand, when continuous lattice curvature is present, as is usually the case in all but the simplest cases of plastic deformation, it is difficult to separate the relative contributions of orientation contrast and diffraction contrast on topographs taken by this method. In principle, the separation could be effected by recording a series of exposures with a wide range of values of b, and it becomes practicable to do so when exposures can be brief, as they can be with synchrotron-radiation sources (see Section 2.7.4.).

For easier separation of orientation contrast and diffraction contrast, and for quicker exposures with conventional X-ray sources, collimated characteristic radiation is used, as in the Berg–Barrett method. Barrett (1945) improved an arrangement earlier described by Berg (1931) by using fine-grain photographic emulsion and by minimizing the ratio b/a, and achieved high topographic resolution (~ 1 μm). The method was further developed by Newkirk (1958, 1959). A typical Berg–Barrett arrangement is sketched in Fig. 2.7.2.1. Usually, the source S is

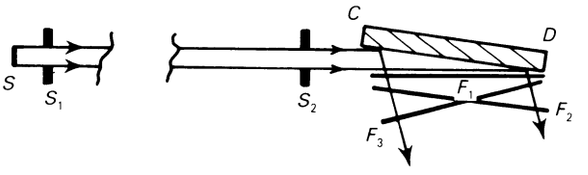

Fig. 2.7.2.1. Berg–Barrett arrangement for surface-reflection topographs.

references